Single-Chip micro-Mote for Microrobotic Platforms

Alex Moreno, Filip Maksimovic, Lydia Lee, Brian Kilberg,
Craig Schindler, Hani Gomez, Daniel Teal,
Dillon Acker-James, Andrew Fearing, Kristofer Pister
Berkeley Sensor & Actuator Center
Department of Electrical Engineering & Computer Sciences
University of California, Berkeley, USA Email: ksjp@berkeley.edu

Jan S. Rentmeister, Jason Stauth
Electrical & Computer Engineering
Dartmouth College
Hanover, NH 03755

***Abstract*—We have demonstrated an embedded microrobot control chip suitable for sub-cm robot platforms. The $2 \times 3 \times 0.3\ mm^3$ 65 nm CMOS chip weighing 4 mg includes a 32 bit Cortex-M0 processor for control, standards-compatible 2.4 GHz RF communication, contact-free optical programming, and sub-cm accurate 3D localization using lighthouse beacons. The chip requires only three wires: power, ground, and a bondwire antenna. No other external components are necessary. With a two-chip solution, we have demonstrated solar-powered operation of 80V MEMS electrostatic inchworm motors suitable for microrobotics.**

***Keywords*—embedded control, mesh network, microrobot, localization, crystal-free, system-on-chip, wireless**

I. Introduction

Microrobot platforms are likely to enable many new defense, intelligence, and commercial applications. Existing microrobot platforms have the potential to run [1], jump [2], and fly [3] autonomously, although at present they are tethered to power and control. Cigarette-sized rockets have the potential to enable rapid distribution of a sensor network, or counter swarms of small UAVs [4], [5]. All of these platforms have a common need for an embedded controller with the capability to run low-level control algorithms, provide diagnostic communication during application development, and provide 2D or 3D location capability. In addition, RF mesh networking is an enabling capability for many robotic applications and non-robotic applications such as industrial process automation and factory automation [6].

Unfortunately, while there are many commercial chips which include a microprocessor and a radio in a sub-cm package, all of these chips require a significant number of external components such as crystal oscillators for time and frequency reference, bypass capacitors for power supplies, a balun for single-ended antennas, etc. As a result, the smallest useful system featuring these commercial chips is typically a printed circuit board with dimensions on the order of a centimeter and weight close to a gram [7]. This is a prohibitively large payload for a sub-cm robot to carry. In 2013 work began in earnest to design a chip that would meet the requirements of microrororobot control and communication with no external components. Funded by DARPA, NSF, and many BSAC member companies over a period of seven years, the chip described below is a result of that effort.

This work was supported in part by the DARPA SHRIMP program under contract HR001119C0047, the NSF PFI:AIR program under grant #1434067, NSF GRFP under grant DGE 1752814, the Berkeley Sensor and Actuator Center, and the Berkeley Wireless Research Center. DISTRIBUTION STATEMENT A. Approved for public release: distribution is unlimited.

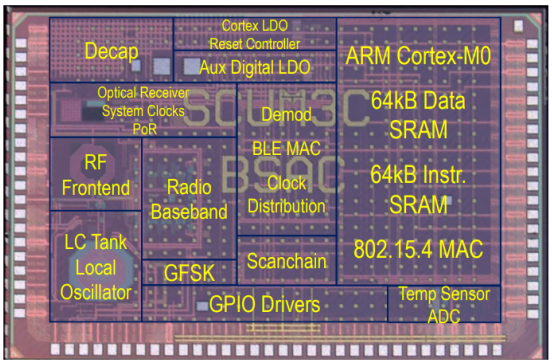

Fig. 1. Annotated die photo of the Single-Chip micro-Mote (SCμM), a chip custom-designed to control microrobots. The single-chip mote is $2{\times}3{\times}0.3\mathrm{mm}^3$ with a mass of $\approx 4.2\mathrm{mg}$.

We present the Single-Chip micro-Mote (SCμM), a $2{\times}3{\times}0.3\ \mathrm{mm}^3$, 4.2 mg chip as-fabricated in 65nm CMOS which contains an integrated crystal-free 802.15.4-compatible radio transceiver, Bluetooth Low Energy (BLE) beacon transmitter, external sensor interface, contactless optical bootloader, and Cortex-M0 microprocessor with 64 kB each of program and data SRAM. SCμM is also capable of centimeter-precision for 3 degrees of freedom (3 DoF) localization using commercially-available lighthouse beacons.

II. Capabilities and Operation

SCμM programs are typically written in C in a standard development environment. Binaries are loaded into SRAM via a USB dongle with both wired and wireless optical programming capability. At boot, the chip consumes roughly 0.35mA. Once software has been loaded and begins executing, this baseline current can be dropped to roughly 0.15mA plus 50μA/MHz times the processor clock frequency. The processor clock frequency can be set from tens of kHz to 20 MHz.

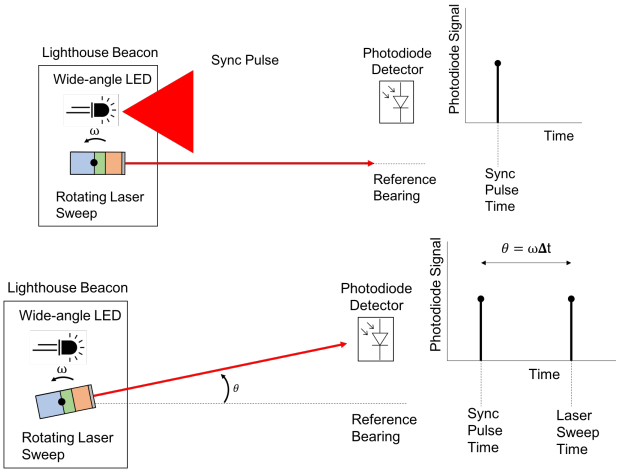

Fig. 2. Lighthouse localization uses temporally-structured light generated by "lighthouse beacons" to localize photodiode-equipped devices. The beacons consist of a wide angle LED and a continuously rotating planar laser scanner. (a.) When the rotating laser scan reaches the reference bearing, the wide angle LED flashes. The photodiode-equipped device detects this pulse and records the time at which it happens. (b.) When the rotating scan eventually reaches the photodiode-equipped device, the device records the time of the scan's arrival. Using the constant angular velocity of the rotating scan and the time difference between the wide angle flash and laser scan, the photodiode device can quickly calculate its relative bearing. [8]

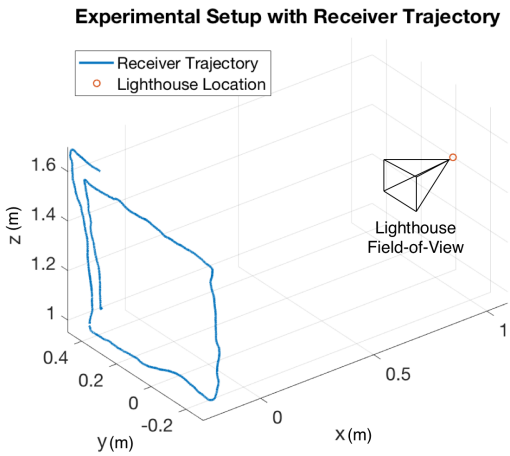

Fig. 3. In the lighthouse tracking experiment, a SCμM was tracked via lighthouse localization as it followed a trajectory. The ground truth trajectory of the chip was tracked simultaneously using an Optitrack motion capture system, which is displayed by the blue line. Since one lighthouse was used, only the azimuth and elevation angles relative to the single lighthouse, could be tracked. Two lighthouses are required for full 3D localization. [8]

A. *Optical Bootloading*

An optical bootloader enables contact-less programming, command reception, and timing calibration of SCμM with an infrared LED or visible laser pointer at a distance of roughly 5cm[8]. The subsystem consists of an integrated photodiode and an analog front-end, as well as a self-timed clock-and-data recovery (CDR) scheme which relies on an analog delay to implement pulse width modulation. This allows a user to load software onto the mote's microprocessor without a physical connection between the programming element and the mote, and it is conducive to the simultaneous programming of multiple motes. The optical bootloader subsystem consumes 640nW standby power and 1.52μW active power with a total area of 16,900μm^2 [8]. The same hardware is used for lighthouse localization (Section II-C).

B. *Standards-compatible RF Communication*

Existing wireless systems-on-chip rely on external components—capacitors, inductors, crystals, and MEMS resonators [9]—to obtain a sufficiently accurate frequency reference for operation, and the necessity of such parts places a lower bound on system cost, size, and weight. By removing these off-chip references and instead using on-chip oscillators for frequency generation with a one-time calibration [10], we achieve IEEE 802.15.4-compatible radio communication and BLE packet transmission with only three external connections—power, ground, and antenna [11].

A wirebond across the chip can be used as an antenna, enabling transmission to cell phones up to a distance of roughly 3 meters. An RSSI of -85 dBm was measured at a distance of 1 m on a previous iteration of the SCμM with the same receiver hardware. The entire chip including the microprocessor consumes less than 2 mW of power during transmission or reception. Transmission power and receive sensitivity for 802.15.4 packets are -10 dBm and -82 dBm.

The ability to wirelessly transmit robot telemetry information during robot development and debugging is quite useful, and the ability to send a wireless trigger to the robot to initiate operations could be useful.

C. *Sub-centimeter 3-DoF Localization*

SCμM has the capability of sub-centimeter-precision 3 degree of freedom (3-DoF) localization, using a COTS lighthouse localization system [12]. This is the first time such a lighthouse localization system has been used to localize a monolithic single-chip wireless system [8]. Lighthouse localization is a form of "outside-in" localization which relies on a "lighthouse beacon" to generate a series of of infrared pulses and laser scans (see Figure 2) [13]. By repurposing the on-chip optical receiver hardware used for optical bootloading (Section II-A) and determining the time between the pulse and the laser scan's reception on-chip, SCμM can calculate its azimuth and elevation with respect to a single beacon. With a commercially available HTC Vive V1 lighthouse base station, we have localized azimuth and elevation with an RMS error of 0.386° and 0.312°, respectively (see Figures 3 and 4) [8]. Because each mote calculates only its own azimuth and elevation, this method scales well to localizing large numbers of motes (or robots) simultaneously. Adding a second lighthouse beacon to this system allows us to triangulate a 3 degree-of-freedom position of SCμM with centimeter accuracy.

Using COTS lighthouse beacons is useful during development and in some application environments. In many applications, however, there will be no pre-existing infrastructure.

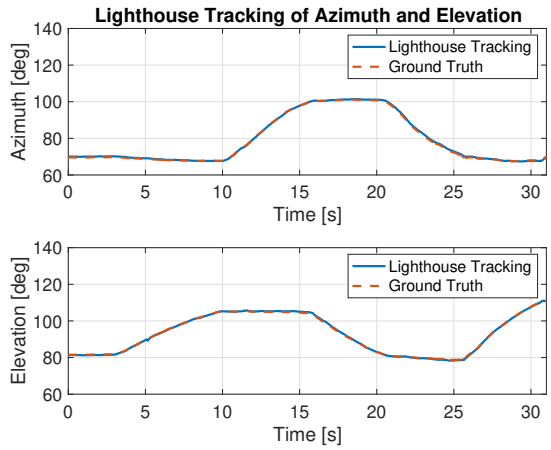

Fig. 4. Results of lighthouse tracking experiment. The ground truth azimuth and elevation angles relative to the lighthouse were calculated using the 3D ground truth trajectory. The RMS error of azimuth and elevation tracking was 0.386 degrees and 0.312 degrees, respectively. [8]

Networks of micro robots may still be able to self-localize however. Using MEMS scanning mirrors it is possible to build laser scanners with a volume and mass compatible with microrobot platforms [14]. By having each robot act as both a beacon and a receiver, the robots localize each other, and only a small number of robots will need to have a sense of their absolute position.

Microrobots will require closed-loop position control to stay on course. The versatility of the platform can be significantly enhanced with computational power greater than hard-coded PID-style control loops. The inclusion of a Cortex-M0 microprocessor integrated with the chip's analog hardware allows for a flexible platform with which to implement control methods, modifiable in software, and configurable without physically contacting the platform (Section II-A).

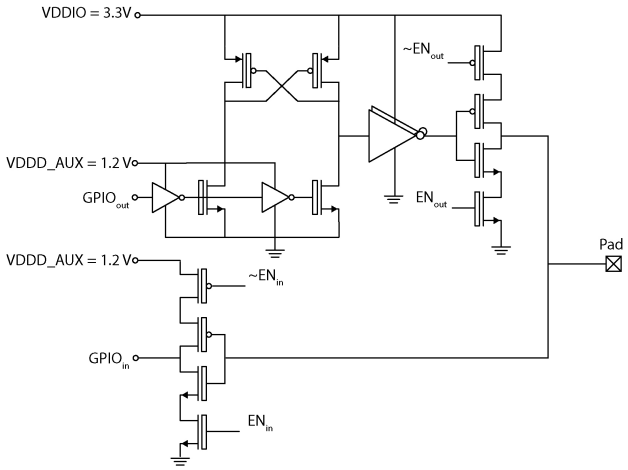

Fig. 5. GPIO circuit schematic

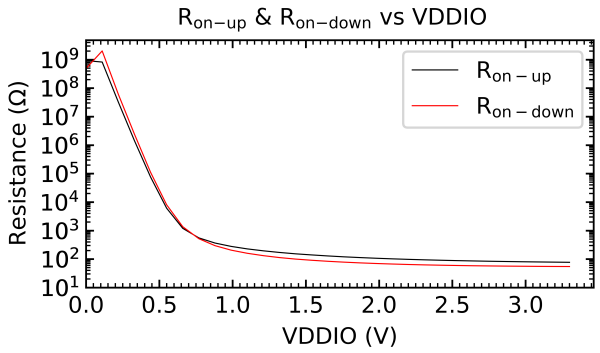

Fig. 6. $\mathrm{GPIO_{output}}$ Resistance vs VDDIO

TABLE I
$\mathrm{GPIO_{output}}$ SPECIFICATIONS

Specification	Value
VDDIO	0.8-3.6 V
VDDAUX	0.8-1.2 V
$\mathrm{F_{max}}$ @ HCLK = 10 MHz	734.25 KHz
$\mathrm{I_{VDDIO\ leakage}}$ @ VDDIO = 3.3 V	4.37 nA
$\mathrm{I_{sink/source}}$ @ VDDIO = 3.3 V	19 mA

D. GPIO

SCμM includes 16 GPIOs whose signals can be routed to and from various sub-systems within the chip and configured via software. Several interrupt inputs are available, as well as an ADC and UART. The IO pad ring voltage is supplied from a separate pin from the battery voltage, and can be driven to at least 3.6 V. The $\mathrm{R_{on}}$ looking up or down at the output of GPO can bee seen in Fig. 6. The schematic of the GPIO drivers can be seen in Fig. 5 The relevant specifications for the GPO can be seen in Table I.

E. Sensors and Sensor Interfacing

SCμM contains an analog-to-digital converter (ADC) with a programmable gain amplifier (PGA) to digitize on-chip and off-chip signals. On-chip sensors include a temperature sensor and voltage supply sensor. The ADC has been used to interface with an H2S gas sensor and a lactate sweat sensor. Wireless transmission of gas sensor information has been demonstrated with just SCμM and the sensor chip and no other components [15]. Serial digital interfacing with external sensors including a commercial nine-axis inertial measurement unit (ICM-20948) has been demonstrated. A MEMS IMU is likely to be critical for microrobot control in practical applications.

In addition to an analog temperature sensor, the chip is able to generate a temperature estimate by taking a ratio of two low frequency oscillators. This is somewhat similar to the technique presented in [16], in which two ring oscillators with different temperature coefficients are counted against one another. The two oscillators on this chip that are compared are the 32 kHz oscillator intended to act as a surrogate for

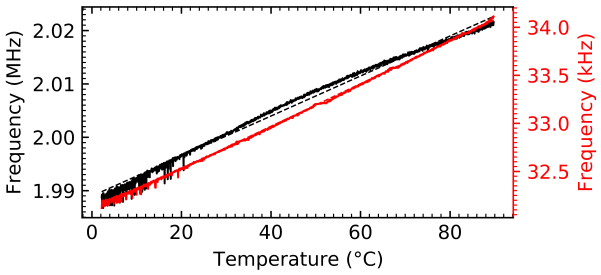

Fig. 7. 32 KHz (red) and 2 MHz (black) Oscillator Frequency vs Temperature

a low-frequency crystal timer, and the 2 MHz oscillator used as the chipping clock for data transmission. The temperature coefficients of the individual oscillators are shown in Fig. 7.

The maximum error on this chip was approximately 2.4 °C, although this varies from chip to chip. The sensor, as well as more information about the implementation, is discussed in [17].

III. Microrobot Actuator Drive and Networking

For low-voltage actuators up to a few tens of mW, SCµM GPOs may be able to drive the actuators directly. For many microrobot actuators, however, the voltage levels required for actuation are much higher than the 3.6V the GPIOs can provide.

A. Two chip high voltage solar-powered MEMS actuator driver

Rentmeister et al. have designed a chip containing several photovoltaic (PV) power supplies and four low-to-high-voltage level shifters in a $3{\times}3\mathrm{mm}^2$ package [18]. Using a 650 V trench-isolated CMOS process, hundreds of PV cells are fabricated on the same chip. Three PV cells in series provides the 1.5 V VBAT to power the SCµM digital system, while six cells in series provides the 3 V VDDIO necessary for the SCµM GPO ring to drive the input to the high-voltage level shifters. 196 PV cells in series generate over 100 V to supply the four level shifters.

In a breadboard demo With illumination from a bright flashlight, the PV chip generated sufficient power for SCµM to boot and be optically programmed. SCµM then ran a simple open-loop finite state machine program that drove two GPOs (powered from the PV chip) with appropriate timing to run an electrostatic inchworm motor. These 3.3 V GPO signals were fed into the level shifters, which were powered by the on-chip PV array. These high voltage waveforms are then used to run the electrostatic inchworm motor on a MEMS microgripper suitable for microrobot and other applications. The gripper is able to produce $15\mathrm{mN}$ (1.5 gram) gripping force[19]. Bypass capacitors were used on the PV supplies, but otherwise the only components in the demo were SCµM, the PV chip, and the MEMS gripper chip. The total volume of the chips and capacitors was under 0.1 cc. We are working towards a centimeter-scale integrated solar-powered wireless microgripper, as shown in Fig. 8 at the bottom.

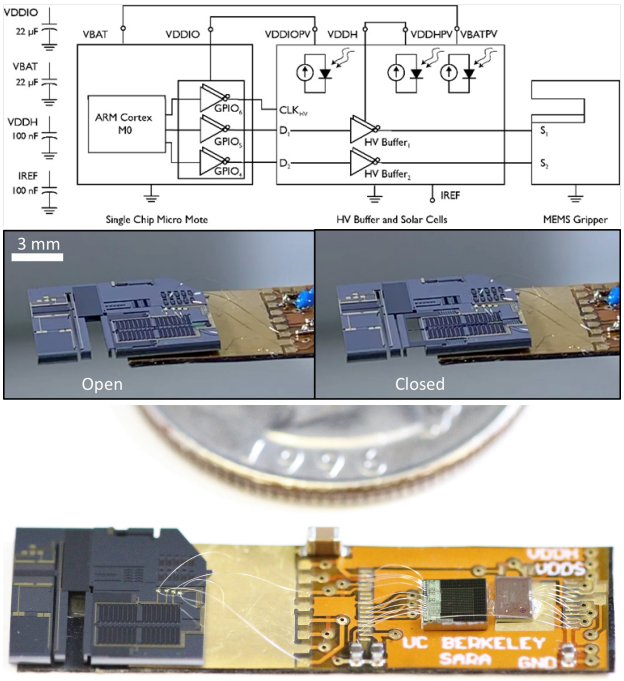

Fig. 8. Top: Setup of SCµM + HV buffer actuating a MEMS gripper at 1mm/s via button trigger. Middle Left: MEMS gripper open. Middle Right: MEMS gripper closed [19]. Bottom (left to right): Assembled Gripper, solar cells and HV buffer, and SCµM

B. Networking

1) OpenWSN and 802.15.4: OpenWSN is an open-source software project which has demonstrated an implementation of the IEEE/IETF standards-compliant 6TiSCH constrained network protocol stack for wireless mesh networks [20]. SCµM was designed to run the OpenWSN IPv6 mesh networking communication stack.

Equipping each microrobot with an OpenWSN-capable radio enables them to form a cooperative mesh network that increases the effective range of the robots communication (beyond that of what would otherwise be a home base) and makes them resilient to RF environments and fading. Using the wireless subsystem on the single-chip mote and an FPGA emulating the on-chip digital hardware, [21] demonstrated the single-chip mote joining an OpenWSN network. Since then, the radio with integrated digital baseband and processor has communicated with Texas Instruments CC2538 802.15.4 radios.

The physical layer that OpenWSN is built on is IEEE 802.15.4, a standard that uses HSS-OQPSK modulation.

Data is sent with a directly modulated LC oscillator where a tunable capacitor is switched in and out of the resonator at the 2 MHz data rate. The receiver is a low-IF superheterodyne architecture with switched-capacitor baseband filtering, a 4-bit analog to digital converter, and a matched filter demodulator. More detail of the implementation is described in [10].

Speaking standards-compatible RF protocols without an external crystal is a difficult challenge [22]. Requirements

for center-frequency accuracy, modulation frequency, bit rate, and inter-packet interval timing are typically measured in tens of parts per million, whereas on-chip oscillator phase noise and frequency error are more often in units of percent. SCμM solves these problems using a combination of circuit techniques and packet-based and network-based dynamic calibration [23], [24]. It is possible for a mote with no initial calibration to learn everything that it needs to know about time and frequency just from the packets flying around in the network that it joins.

2) Bluetooth: Some Bluetooth Low Energy (BLE) functionality is available in SCμM. Beacon transmissions with sensor payload data are received routinely by cell phones. Reception range depends on the antenna used, with a range of several meters using a wirebond antenna across the chip, and a range of several tens of meters using a commercial antenna. Reception of BLE packets by the mote has not yet been demonstrated. The radio can move between 802.15.4 and BLE modes in a matter of milliseconds, allowing a node to relay data out of an 802.15.4 mesh to a nearby cell phone.

C. Discussion

SCuM3C was designed for micro robot control, networking, and localization. Software development is still in progress, and should enable swarms of robots to form a mesh network and exchange information to help them achieve their goals. Powering from an array of solar cells on a similar-sized IC demonstrates that wireless powering is possible, and that high-voltage MEMS motors can be controlled from a 10 mg electronics package. Future improvements should increase the range of output voltages and currents that can be driven, and reduce the size of a single-chip mote still further. A 1 mm^2 version of the chip has been designed [25].

REFERENCES

[1] D. S. Contreras and K. Pister, "A six-legged MEMS silicon robot using multichip assembly," in *Solid State Sensors and Actuators Workshop, Hilton Head*, 2018.

[2] C. B. Schindler, J. T. Greenspun, H. C. Gomez, and K. S. Pister, "A jumping silicon microrobot with electrostatic inchworm motors and energy storing substrate springs," in *2019 20th International Conference on Solid-State Sensors, Actuators and Microsystems & Eurosensors XXXIII (TRANSDUCERS & EUROSENSORS XXXIII)*. IEEE, 2019, pp. 88–91.

[3] D. S. Drew, N. O. Lambert, C. B. Schindler, and K. S. Pister, "Toward controlled flight of the ionocraft: a flying microrobot using electrohydrodynamic thrust with onboard sensing and no moving parts," *IEEE Robotics and Automation Letters*, vol. 3, no. 4, pp. 2807–2813, 2018.

[4] A. M. Rauf, B. G. Kilberg, C. B. Schindler, S. A. Park, and K. S. Pister, "Towards aerodynamic control of miniature rockets with mems control surfaces," in *IEEE MEMS*, 2020.

[5] D. S. Drew, B. Kilberg, and K. S. Pister, "Future mesh-networked pico air vehicles," in *2017 International Conference on Unmanned Aircraft Systems (ICUAS)*. IEEE, 2017, pp. 1075–1082.

[6] T. Watteyne, V. Handziski, X. Vilajosana, S. Duquennoy, O. Hahm, E. Baccelli, and A. Wolisz, "Industrial wireless ip-based cyber–physical systems," *Proceedings of the IEEE*, vol. 104, no. 5, pp. 1025–1038, 2016.

[7] C. B. Schindler, D. S. Drew, B. G. Kilberg, F. M. Campos, S. Yanase, and K. S. Pister, "Mimsy: The micro inertial measurement system for the internet of things," in *2019 IEEE 5th World Forum on Internet of Things (WF-IoT)*. IEEE, 2019, pp. 329–334.

[8] B. Wheeler, A. Ng, B. Kilberg, F. Maksimovic, and K. Pister, "A low-power optical receiver for contact-free programming and 3d localization of autonomous microsystems," in *IEEE UEMCON*, 2019.

[9] D. Griffith, P. T. Røine, T. Kallerud, B. Goodlin, Z. Hughes, and E. T. Yen, "A $\pm$10ppm $-$40 to 125°C BAW-Based Frequency Reference System for Crystal-less Wireless Sensor Nodes," in *2017 IEEE International Symposium on Circuits and Systems (ISCAS)*, 5 2017, pp. 1–4.

[10] F. Maksimovic, B. Wheeler, D. C. Burnett, O. Khan, S. Mesri, I. Suciu, L. Lee, A. Moreno, A. Sundararajan, B. Zhou *et al.*, "A crystal-free single-chip micro mote with integrated 802.15. 4 compatible transceiver, sub-mw ble compatible beacon transmitter, and cortex m0," in *VLSI 2019*. IEEE, 2019, pp. C88–C89.

[11] F. Maksimovic, B. Wheeler, D. Burnett, L. Lee, S. Mesri, O. Khan, A. Niknejad, and K. Pister, "Standards Compatible RF Networks without Crystals: A three-pin BLE beacon-on-a-chip," in *Arm Research Summit 2019*, 9 2019.

[12] Vive lighthouse base station, https://www.vive.com/us/accessory/base-station, retrieved 1/10/2020.

[13] K. Römer, "The lighthouse location system for smart dust," in *Proceedings of the 1st international conference on Mobile systems, applications and services*. ACM, 2003, pp. 15–30.

[14] M. Last and K. Pister, "An 8 mm3 digitally steered laser beam transmitter," in *IEEE/LEOS Intl. Conf. Optical MEMS*, 2000.

[15] D. C. Burnett, H. M. Fahad, L. Lee, F. Maksimovic, B. Wheeler, O. Khan, A. Javey, and K. S. J. Pister, "Two-chip wireless H_2S gas sensor system requiring zero additional electronic components," in *Transducers 2019*, 6 2019, pp. 1222–1225.

[16] S. Jeong, Z. Foo, Y. Lee, J.-Y. Sim, D. Blaauw, and D. Sylvester, "A fully-integrated 71 nW CMOS temperature sensor for low power wireless sensor nodes," in *IEEE Journal of Solid State Circuits*, 2014, pp. 1682–1693.

[17] T. Yuan, F. Maksimovic, and K. Pister, "Temperature calibration on a crystal-free mote," in *Submitted to 2020 IEEE World Forum on Internet of Things*, April 2020.

[18] J. S. Rentmeister, K. Pister, and J. T. Stauth, "A 120-330 V, sub-μA, optically powered microrobotic drive IC for DARPA SHRIMP," in *GOMACTech*, 2020.

[19] C. Schindler, H. Gomez, D. Acker-James, D. Teal, W. Li, and K. Pister, "15 millinewton force, 1 millimeter displacement, low-power MEMS gripper," in *IEEE MEMS*, 2020.

[20] T. Watteyne, X. Vilajosana, B. Kerkez, F. Chraim, K. Weekly, Q. Wang, S. Glaser, and K. Pister, "Openwsn: a standards-based low-power wireless development environment," *Transactions on Emerging Telecommunications Technologies*, vol. 23, no. 5, pp. 480–493, 2012.

[21] T. Chang, T. Watteyne, B. Wheeler, F. Maksimovic, O. Khan, S. Mesri, L. Lee, I. Suciu, X. Vilajosana, and K. Pister, "6TiSCH on SCμM:running a synchronized protocol stack without crystals," in *ACMEmbedded Wireless Systems and Networks*, 2020.

[22] D. C. Burnett, B. Wheeler, L. Lee, F. Maksimovic, A. Sundararajan, O. Khan, and K. S. Pister, "Cmos oscillators to satisfy 802.15. 4 and bluetooth le phy specifications without a crystal reference," in *2019 IEEE 9th Annual Computing and Communication Workshop and Conference (CCWC)*. IEEE, 2019, pp. 0218–0223.

[23] I. Suciu, F. Maksimovic, D. Burnett, O. Khan, B. Wheeler, A. Sundararajan, T. Watteyne, X. Vilajosana, and K. Pister, "Experimental clock calibration on a crystal-free mote-on-a-chip," in *IEEE INFOCOM 2019-IEEE Conference on Computer Communications Workshops (INFOCOM WKSHPS)*. IEEE, 2019, pp. 608–613.

[24] I. Suciu, F. Maksimovic, B. Wheeler, D. C. Burnett, O. Khan, T. Watteyne, X. Vilajosana, and K. S. Pister, "Dynamic channel calibration on a crystal-free mote-on-a-chip," *IEEE Access*, vol. 7, pp. 120 884–120 900, 2019.

[25] D. C. Burnett, B. Kilberg, R. Zoll, O. Khan, and K. S. Pister, "Tapeout class: Taking students from schematic to silicon in one semester," in *2018 IEEE International Symposium on Circuits and Systems (ISCAS)*. IEEE, 2018, pp. 1–5.